

Adventures in Multi-Omics I: Combining heterogeneous data sets via relationships matrices

Deniz Akdemir*, Julio Isidro Sánchez

Received: date / Accepted: date

Abstract In this article, we propose a covariance based method for combining partial data sets in the genotype to phenotype spectrum. In particular, an expectation-maximization algorithm that can be used to combine partially overlapping relationship/covariance matrices is introduced. Combining data this way, based on relationship matrices, can be contrasted with a feature imputation based approach. We used several public genomic data sets to explore the accuracy of combining genomic relationship matrices. We have also used the heterogeneous genotype/phenotype data sets in the <https://triticeaetoolbox.org/> to illustrate how this new method can be used in genomic prediction, phenomics, and graphical modeling.

Keywords Multi-Omics · Phenomics · Breeding · Complex traits · Genomic selection · Genome-wide markers · Kernel-regression · Multiple kernel learning · Mixed models · Imputation · Covariance Estimation · Expectation-Maximization

Key message: Several covariance matrices obtained from independent experiments can be combined as long as these matrices are partially overlapping. We demonstrate the usefulness of this methodology with examples in combining data from several partially linked genotypic and phenotypic experiments.

Conflict of interest: The authors declare that there is no conflict of interest.

Author contribution statement:

- DA: Conception or design of the work, statistics, programs, and simulations, drafting the article, critical revision of the article.
- JIS: Drafting the article, critical revision of the article.

1 Introduction

The area of genomic prediction, i.e. predicting an organism's phenotype using genetic information [Meuwissen et al., 2001], is a cutting edge tool. It is used by

This research was supported by WheatSustain.

* Corresponding author: D Akdemir
University College Dublin, Ireland
E-mail: deniz.akdemir.work@gmail.com

many breeding companies, because it improves three out of the four factors affecting the breeder's equation [Hill and Mackay, 2004]. It reduces generation interval, improves accuracy of selection and increase selection intensity for a fixed budget when comparing with marker-assisted selection or phenotypic selection [Desta and Ortiz, 2014, Heffner et al., 2011, 2010, Juliana et al., 2018, de los Campos et al., 2013]. Genomic selection (GS) and prediction are in a continuous progressing tool that promises to help to meet the human food challenges in the next decades [Crossa et al., 2017]. Genome-wide associating mapping studies, which originated in human genetics [Bodmer, 1986, Risch and Merikangas, 1996, Visscher et al., 2017], has also become a routine in plant breeding [Gondro et al., 2013].

The rapid scientific progress in these genomics studies was due to the decrease in genotyping costs by the development of next generation sequencing platforms after 2007 [Mardis, 2008a,b]. High-throughput instruments are routinely used in laboratories in basic science applications, which led to the democratization of genome-scale technologies. The biological data generated in the last few years have growth exponentially which led to a high dimensional and unbalanced nature of the 'omics' data, in the forms of marker and sequence information; expression, metabolomics, microbiome data, classical phenotype data, image-based phenotype data [Bersanelli et al., 2016]. Private and public breeding programs, as well as companies and universities, have developed different genomics technology which has resulted in the generation of unprecedented levels of sequence data, which bring new challenges in terms of data management, query, and analysis.

It is clear that detailed phenotype data, combined with increasing amounts of genomic data, have an enormous potential to accelerate the identification of key traits to improve our understanding of quantitative genetics [Crossa et al., 2017]. Nevertheless, one of the challenges that still need to be addressed is the incompleteness inherent in these data, i.e., several types of genomic/phenotypic information which might each covering only a few of the genotypes under study [Berger et al., 2013]. Data harmonization enables cross-national and international comparative research, as well as allows the investigation of whether or not data sets have similarities. In this paper, we address the complex issue of the high degree of dimensional and unbalanced nature of the omics data by studying how we can combine data generated from different sources and facilitating data integration and interdisciplinary research. The increase of sample size and the improvement of generalizability and validity of research results constitute the most significant benefits of the harmonization process. The ability to effectively harmonize data from different studies and experiments facilitates the rapid extraction of new scientific knowledge.

One way to approach the incompleteness and the disconnection among datasets is to combine the relationship information learned from these dataset. The statistical problem addressed in this paper is the calculation of a combined covariance matrix from incomplete and partially-overlapping pieces of covariance matrices that were obtained from independent experiments. We assume that the data is a random sample of partial covariance matrices from a Wishart distribution, then we derive the expectation-maximization algorithm for estimating the parameters of this distribution. According to our best knowledge no such statistical methodology exists, although the proposed method has been inspired by similar methods such as (conditional) iterative proportional fitting for the Gaussian distribution [Cramer, 1998, 2000] and a method for combining a pedigree relationship matrix

and a genotypic matrix relationship matrix which includes a subset of genotypes from the pedigree-based matrix [Legarra et al., 2009] (namely, the H-matrix). The applications in this paper are chosen in the area of plant breeding and genetics. However, the statistical method is applicable much beyond the described examples in this article.

2 Methods and Materials

2.1 Statistical methods for combining incomplete data

2.1.1 Imputation

The standard method of dealing with heterogeneous data involves the imputation of features [Shrive et al., 2006]. If the data sets to be combined overlap over a substantial number of features then the unobserved features in these data sets can be accurately imputed based on some imputation method [Rutkoski et al., 2013].

Imputation step can be done using many different methods: Several popular approaches include random forest [Breiman, 2001] imputation, expectation maximization based imputation [Endelman, 2011], low-rank matrix factorization methods that are implemented in the R package [Hastie and Mazumder, 2015]. In addition, parental information can be used to improve imputation accuracies [Nicolazzi et al., 2013, Gonen et al., 2018, VanRaden et al., 2015, Browning and Browning, 2009]. In this study, we used the low-rank matrix factorization method in all of the examples which included an imputation step. The selection of this method was due to computational burden of the other alternatives.

2.1.2 Combining genomic relationship matrices

In this section, we describe the Wishart EM-Algorithm for combining partial genetic relationship matrices¹.

Wishart EM-Algorithm for Estimation of a Combined Relationship Matrix from Partial Samples

Let $A = \{a_1, a_2, \dots, a_m\}$ be the set of not necessarily disjoint subsets of genotypes covering a set of K (i.e., $K = \cup_{i=1}^m a_i$) with total n genotypes. Let $G_{a_1}, G_{a_2}, \dots, G_{a_m}$ be the corresponding sample of genetic relationship matrices.

Starting from an initial estimate $\Sigma^{(0)} = \nu\Psi^{(0)}$, the Wishart EM-Algorithm repeats updating the estimate of the genetic relationship matrix until convergence:

$$\Psi^{(t+1)} = \frac{1}{\nu m} \sum_{a \in A} P_a \begin{bmatrix} G_{aa} & G_{aa}(B_{b|a}^{(t)})' \\ B_{b|a}^{(t)}G_{aa} & \nu\Psi_{bb|a}^{(t)} + B_{b|a}^{(t)}G_{aa}(B_{b|a}^{(t)})' \end{bmatrix} P_a' \quad (1)$$

¹ In what follows, we will refer to genetic relationship matrices that measure how genotypes are related (See Supplementary Section 5.3 for a description of how to calculate a genetic relationship matrix from genome-wide markers (genomic relationship matrix)). However, a theme in this article is that a genetic relationship matrix is a special kind of covariance matrix. Therefore, the same arguments below apply to covariance matrices that measure the relationship between traits or features.

where $B_{b|a}^{(t)} = \Psi_{ab}^{(t)}(\Psi_{aa}^{(t)})^{-1}$, $\Psi_{bb|a}^{(t)} = \Psi_{bb}^{(t)} - \Psi_{ab}^{(t)}(\Psi_{aa}^{(t)})^{-1}\Psi_{ba}^{(t)}$, a is the set of genotypes in the given partial genomic relationship matrix and b is the set difference of K and a . The matrices P_a are permutation matrices that put each matrix in the sum in the same order. The initial value, $\Sigma^{(0)}$ is usually assumed to be an identity matrix of dimension n . The estimate $\Psi^{(T)}$ at the last iteration converts to the estimated genomic relationship with $\Sigma^{(T)} = \nu\Psi^{(T)}$.

A weighted version of this algorithm can be obtained replacing G_{aa} in Equation 1 with $G_{aa}^{(w_a)} = w_a G_{aa} + (1 - w_a)\nu\Psi^{(T)}$ for a vector of weights $(w_1, w_2, \dots, w_m)'$.

Derivation of the Wishart-EM algorithm and its asymptotic errors are given in Supplementary.

2.2 Materials: Data sets and Experiments.

In this section, we describe the data sets and the experiments we have designed to explore and exploit the Wishart EM-Algorithm.

Note that the examples in the main text involve real data sets and validation with such data can only be as good as the ground truth known about the underlying system. We also included several simulation studies in the supplementary (Supplementary Example 1 and 2) using simulated data to show that the algorithm performs as expected (maximizes the likelihood and provides a 'good' estimate of the parameter values) when the ground truth is known.

Example 1- Potato Data set; when imputation is not an option. Anchoring independent pedigree-based relationship matrices using a genotypic relation matrix

The Wishart EM-Algorithm can be used when the imputation of the original genomic features is not feasible. For instance, it can be used to combine partial pedigree-based relationship matrices with marker-based genomic relationship matrices. In this example, we demonstrate that genomic relationship matrices can be used to connect several pedigree-based relationship matrices.

The data set is cited in [Endelman et al., 2018] and is available in the R Package AGHmatrix [Rampazo Amadeu et al., 2016]. It consists of the pedigree of 1138 potato genotypes, 571 of these genotypes also have data for 3895 tetraploid markers. The pedigree-based relationship matrix A was calculated with R package AGHmatrix [Rampazo Amadeu et al., 2016] using pedigree records, there were 185 founders (clones with no parent).

At each replication of the experiment, two non-overlapping pedigree-based relationship matrices each with the sample size $N_{ped} \in \{100, 150, 250\}$ genotypes selected at random from the were 571 genotypes were generated. In addition, a genotypic relationship matrix was obtained for a random sample of $N_{geno} \in \{20, 40, 80\}$ genotypes selected at random half from the genotypes in the first pedigree and a half from the genotypes from the second pedigree. These genetic relationship matrices were combined to get a combined genetic relationship matrix (See Figure 1). This combined relationship matrix was compared to the pedigree-based relationship matrix of the corresponding genotypes using mean squared errors and Pearson's correlations. This experiment was repeated 30 times for each N_{geno}, N_{ped} pair.

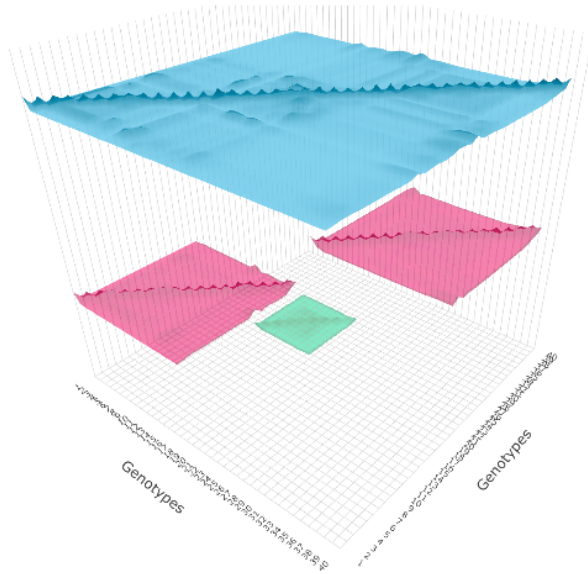


Fig. 1 Potato data set: At each replication of the experiment, two non-overlapping pedigree-based relationship matrices each with N_{ped} (pedigree) genotypes selected at random from the were 571 genotypes were generated. In addition, a genomic relationship matrix was obtained for a random sample of genotypes $N_{geno}2$ selected at random half from the genotypes in the first pedigree and a half from the gebotypes from the second pedigree. These relationship matrices were combined to get a combined relationship matrix. In this figure, for simplicity, we took $N_{ped} = 20$, and $N_{geno} = 5$. Two pedigree-based relationship matrices are in purple, the genotypic relationship matrix is in green and the combined relationship matrix is in blue.

Example 2 - Rice data set. Combining independent low density marker data sets

Rice data set was downloaded from www.ricediversity.org. After curation, the marker data set consisted of 1127 genotypes observed for 387161 markers.

In each instance of the experiment, the number of kernel $N_{Kernel} \in \{3, 5, 10, 20\}$ marker data sets with 200 genotypes and 2000 markers were created by randomly sampling the genotypes and markers in each genotype file. These data sets were combined using the Wishart EM-Algorithm and also by imputation to give two genomic relationship matrices. For the totality of genotypes in these combined data sets, we also randomly sampled 2000, 5000 or 10000 markers and calculated the genomic relationships based on these marker subsets. All of these genomic relationship matrices were compared with the corresponding elements of the relationship matrix based on the entire genomic data by calculating the mean

squared error between the upper diagonal elements including the diagonals. This experiment was repeated 20 times.

Example 3 - Wheat Data at Triticale Toolbox. Combining genomic data sets to use in genomic prediction.

This example involves estimating breeding values for seven economically important traits for 9102 wheat lines obtained by combining 16 publicly available genotypic data sets. The genotypic and phenotypic data were downloaded from the triticale toolbox database. Each of the marker data sets was pre-processed to produce the corresponding genomic relationship matrices. Table 1 and Supplementary Figure S6 describes the phenotypic records and number of distinct genotypes for each trait.

Table 1 Marker data sets from Triticale Toolbox: Labels and names for the data sets, number of genotypes and markers in each of the selected 16 genotypic data sets.

Label	Data	# Genotypes	# Markers
d1	2012_SRWW_ElitePanel	276	90782
d2	2014_HAPMAP	53	180198
d3	2014_SRWW_YNVP	307	109073
d4	2014_TCAPABBSRWMID	365	100340
d5	CornellMaster_2013	1128	18846
d6	Dart_NebDuplicates_2010	278	1970
d7	HWWAMP_2013	288	32288
d8	HWWAMP_2014	311	265551
d9	NSGC9k.spring	2196	5303
d10	NSGC9k.winter	1674	5010
d11	TCAP90k_HWWAMP_SPRN	20	16842
d12	TCAP90k_LeafRust	339	24610
d13	TCAP90k_NAMparents	60	25851
d14	TCAP90k_SpringAm	248	24343
d15	TCAP90k_SWW	317	24978
d16	WWDP9k	2258	6232

Using the combined relationship matrix we can build genomic prediction models. To test the performance of predictions based on the combined relationship matrix, we have formulated two scenarios. The intersection of genotypes among the 16 genotypic experiments is showed in Figure 2 and the intersection of common markers among genotypic experiments in Figure 3.

– Cross-validation scenario 1

The first scenario involved a 10 fold cross-validation based on a random split of the data. For each trait, the available genotypes were split into 10 random folds. The GEBVs for each fold were estimated from a mixed model (see Supplementary Section 5.4 for a description of this model) that was trained on the phenotypes available for the remaining genotypes. The accuracy of the predictions was evaluated by calculating the correlations between the GEBVs and the observed trait values.

- **Cross-validation scenario 2** The second Cross-validation scenario involved leaving out the phenotypic records corresponding genotypes in one of the 16 genomic data sets followed by estimation of the trait values for these genotypes based on a mixed model trained on the remaining genotypes and phenotypic records. This scenario was used for each trait, and the accuracies were evaluated by calculating the correlations between the estimated and the observed trait values within each group.

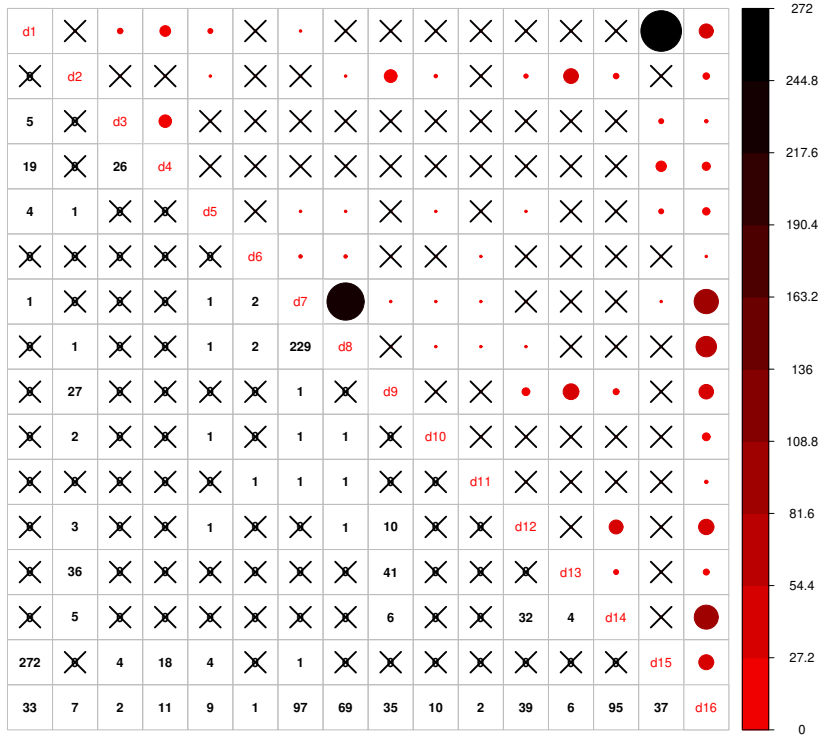


Fig. 2 Triticale data set: Intersection of genotypes among 16 genotypic experiments. The number of common genotypes among the 16 genotypic data sets are given on the lower diagonal, no intersection is marked by 'X'. Upper diagonal of the figure gives a graphical representation of the same, larger circles represent higher number of intersections.

Example 4 - Wheat Data at Triticale Toolbox. Combining Phenotypic Experiments

The Wishart EM-Algorithm can also be used to combine correlation matrices² obtained from independent phenotypic experiments. One-hundred forty four phenotypic experiments involving 95 traits in total were selected from 2084 trials and 216 traits available at the Triticale Toolbox. In this filtered set of trials, each trial and trait combination had at least 100 observations and two traits. Furthermore, the percentage of missingness in these data sets was at most 70%. The mean and the median of the number of traits in these trials were 5.9 and 4 correspondingly (See Figure 5 and Supplementary Figure S5).

The correlation matrix for the traits in each trial was calculated and then combined using the Wishart EM-Algorithm. The resulting covariance matrix was used in learning a directed acyclic graph (DAG) using the qgraph R Package [Epskamp et al., 2012].

A more advanced example that involved combining the phenotypic correlation matrices from oat (78 correlation matrices), barley (143 correlation matrices) and wheat (144 correlation matrices) data sets downloaded and selected in a simi-

² We used correlations instead of covariances because the phenotypic experiments were very heterogeneous in terms of the variances of the different traits.

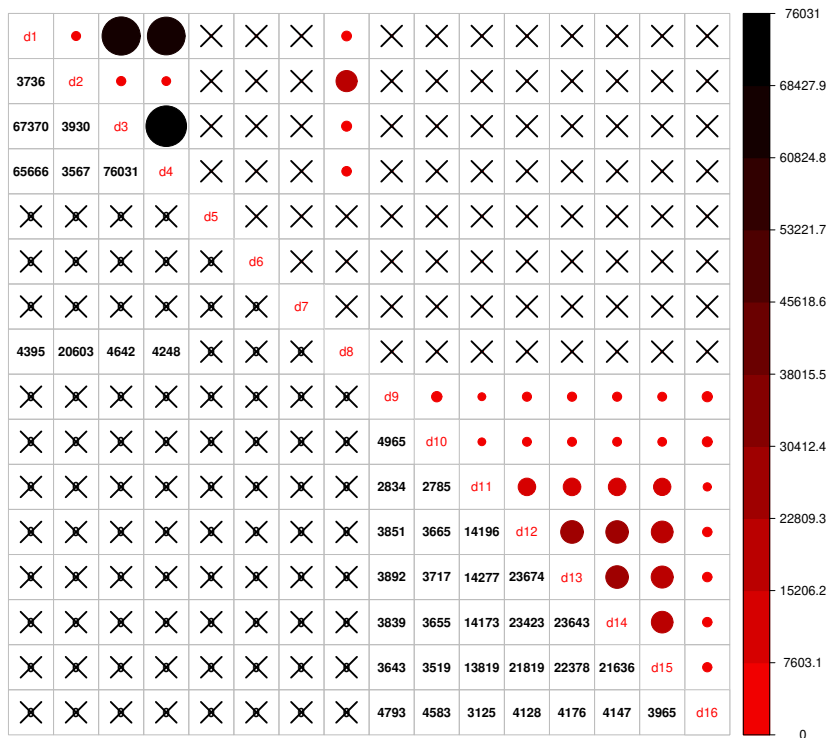


Fig. 3 Triticale data set: Intersection of markers among 16 genotypic experiments. The number of common markers among the 16 genotypic data sets are given on the lower diagonal, no intersection is marked by 'X'. Upper diagonal of the figure gives a graphical representation of the same thing.

lar way as above were combined to obtain the DAG involving 196 traits in the Supplementary (Supplementary Example 6.1).

3 Results

Example 1- When imputation is not an option: Anchoring independent pedigree-based relationship matrices using a genotypic relation matrix - Potato Data

Figure 6 shows the correlation correlation and MSE results as either of the sizes of the pedigree matrices and the number of genotypes in the genomic relationship matrices increases. The MSE results for these experiments ranged from 0.001 to 0.03 with a mean of 0.009, and the correlation values ranged from 0.22 to 0.98 with a mean of 0.78.

Example 2 - Rice data set. Combining independent low density marker data sets

The MSE and correlation results for this experiment are given in Figure 7. In general, as the number of independent data sets increases the accuracy of the all of the methods/scenarios increases (decreasing MSEs and increasing correlations). In

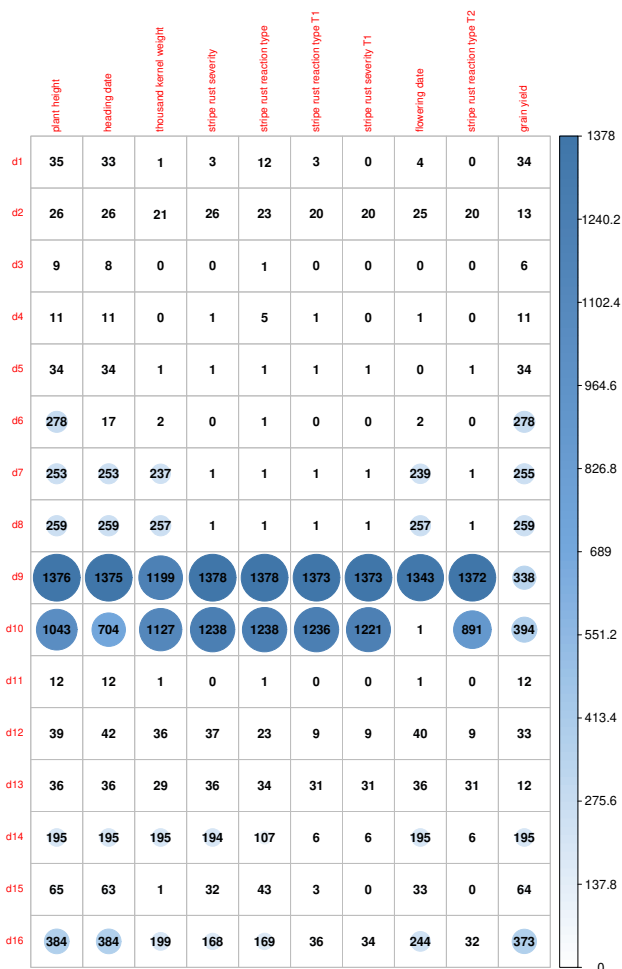


Fig. 4 Triticale data set: Availability of phenotypic data for the genotypes in 16 genotypic data sets for 10 traits. These were the traits with most phenotypic records for the genotypes in the 16 genotypic data sets.

general, the accuracy of the Wishart EM-algorithm in terms of MSEs ranged from 0.0003 to 0.002 with a mean value of 0.0007. The accuracies measured in correlation ranged from 0.989 to 0.998 with a mean value of 0.995. For the imputation based method MSEs ranged from 0.014 to 0.032 (mean 0.019) and the correlations ranged from 0.805 to 0.970 (mean 0.920).

Figure 8 displays the scatter plot of full genomic relationship matrix (obtained using all 387161 markers) against the one obtained by combining a sample of partial relationship matrices (200 randomly selected genotypes and 2000 randomly selected markers each) over varying numbers of samples (3, 5, 10, 20, 40, and 80 partial relationship matrices). Observed parts (observed-diagonal and observed non-diagonal) of the genomic relationship matrix can be predicted with high accuracy and no bias. As the sample size increase, the estimates get closer to the one

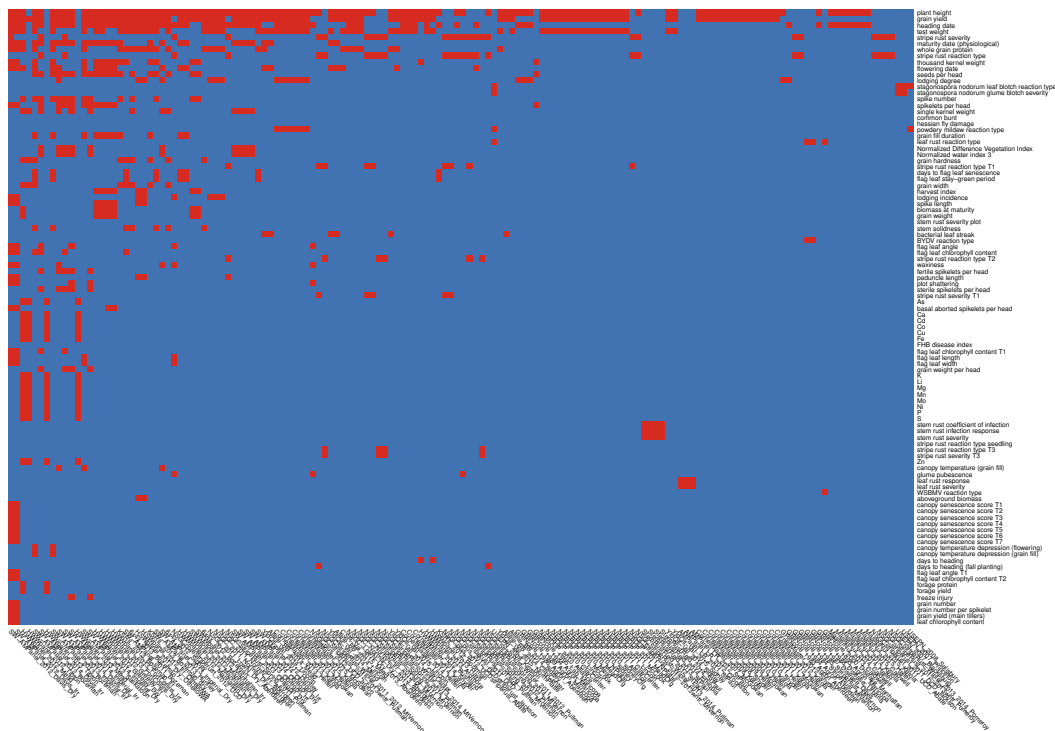


Fig. 5 Availability of data in 144 phenotypic trials and 95 traits at Triticale Toolbox for wheat. Red shows available data, blue shows unavailable data. The traits and trials are sorted based on availability. Plant height was the most commonly observed trait followed by grain yield.

obtained using all of the data. We observe that the estimates of the unobserved parts of the relationship are biased towards zero but this bias quickly decreases as the sample size increases.

Example 3 - Wheat Data at Triticale Toolbox. Combining genomic data sets to use in genomic prediction

The results summarized by Figure 9 indicate that when a random sample of genotypes are selected for the test population the accuracy of the genomic predictions using the combined genomic relationship matrix can be high (Cross-validation scenario 1). Average accuracy for estimating plant height was about 0.68, and for yield 0.58. Lowest accuracy values were for test weight with a mean value of 0.48.

The performance decreases significantly if we use between population predictions (Cross-validation scenario 2). Certain populations were harder to predict, for example, d5, d6, d9. On the other hand, some populations were easier to predict, for example, d12-d16. Average accuracy for estimating plant height was about 0.30, for yield 0.28.

Example 4 - Wheat Data at Triticale Toolbox- Combining Phenotypic Experiments In this example, we combined correlation matrices obtained from independent phenotypic experiments. Figures 10 and S3 displayed the correlation

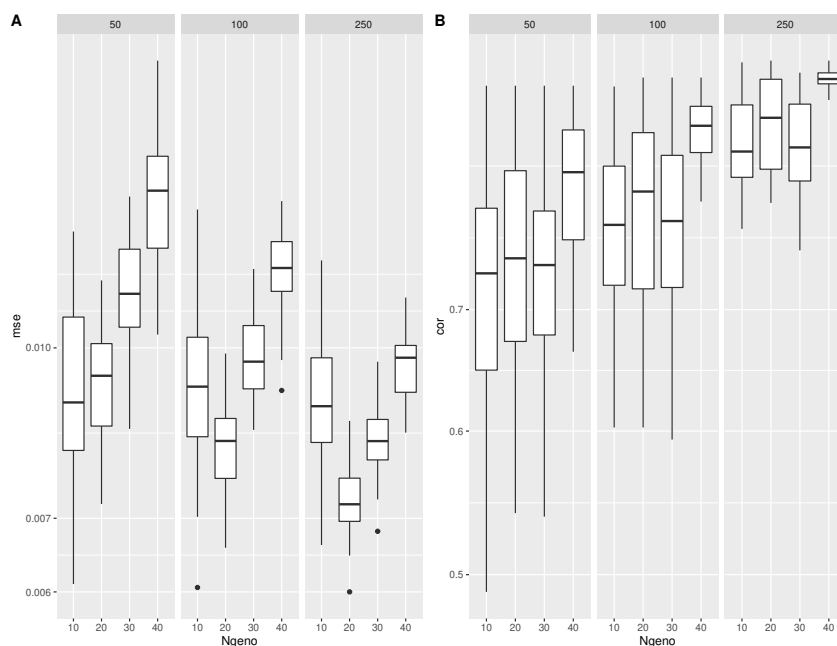


Fig. 6 MSE and correlation values for the unobserved part of the pedigree-based relationship matrix inferred by combining two non-overlapping pedigree-based relationship matrices (of sizes 50, 100, or 250 each) and a genotypic relationship matrix that had 10, 20, 30 or 40 genotypes in each of the pedigrees. Here, **CK** stands for combined relationship matrix with the Wishart EM-algorithm. **Imp** stands for the the relationship matrix obtained after imputation. **2000**, **5000**, **10000** refer to the relationship matrices obtained by using 2000, 5000, or 1000 markers correspondingly.

matrix for the traits in a directed acyclic graph (DAG) and in a heatmap, respectively. In Figure 10 each node represents a trait and each edge represents a correlation between two traits. One of the strength on this representation, is that you can elucidate the correlation between traits that you did not measured in your experiment. For example, from all the traits, grain width (grnwd) and above ground biomass (ab_g_bm) are positive correlated (blue arrows) with grain yield. In turn, grwd is highly positive correlated with biomass at maturity (bm.am) but negative correlated with harvest index (hrvi). Negative correlations (red) can also be observed among traits. Traditional inverse correlations such as protein (wh_gp) and grwd can be also observed.

Combining datasets by correlation matrices also help to group traits. Figure S3 shows two groups of positively traits. The traits in these two groups are positively correlated within the group but negatively correlated with traits in the other group. For example, we see that yield related traits such as traits grain yield, grain weight, harvest index, etc,... are positively correlated. On the other hand these traits are negatively correlated with disease related traits such as bacterial leaf streak, stripe rust traits and also with quality traits such as protein and nutrient content.

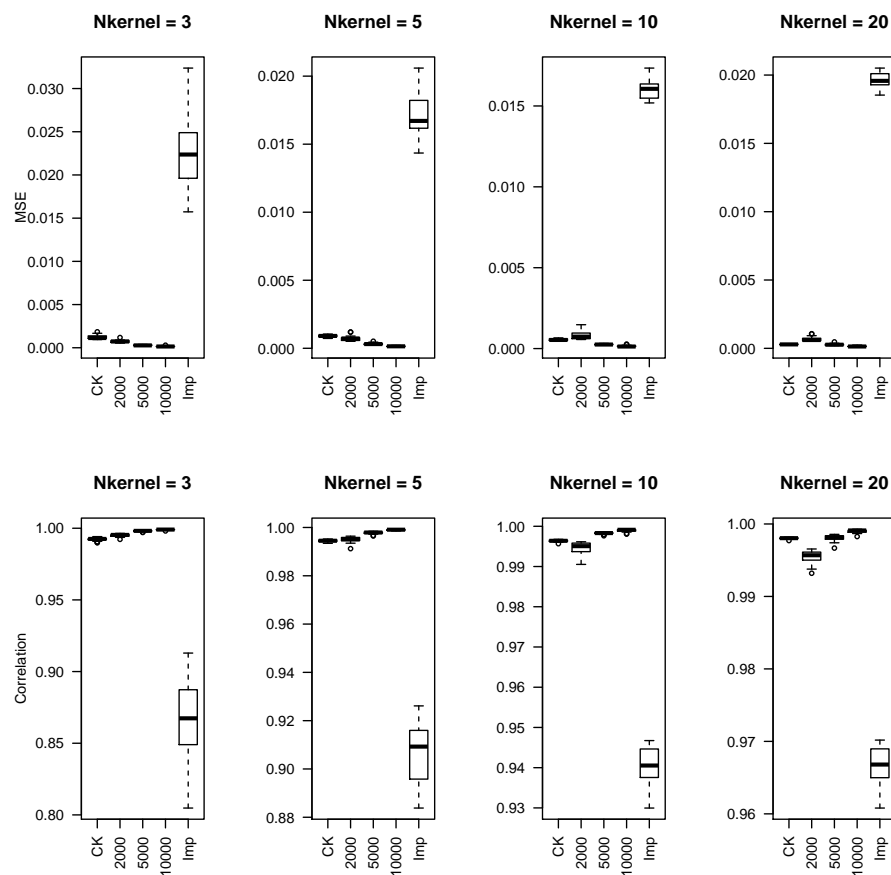


Fig. 7 Rice data set: MSEs and correlations between the estimated and full genomic relationship matrices. The combined matrix predicts the structure of the population more accurately than the relationship matrix obtained by imputing the genomic features.

4 Discussion and conclusions

Genomic data are now relatively inexpensive to collect and phenotypes remain to be the primary way to define organisms. Many genotyping technologies exist and these technologies evolve which leads to heterogeneity of genomic data across independent experiments. Similarly, phenotypic experiments, due to the high relative cost of phenotyping, usually can focus only on a set of key traits of interest. Therefore, when looking over several phenotypic data sets, the usual case is that these data sets are extremely heterogeneous and incomplete, and the data from these experiments accumulate in databases.

This presents a challenge but also an opportunity to make the most of genomic/phenotypic data in the future. In the long term, such databases of genotypic and phenotypic information will be invaluable to scientists as they seek to

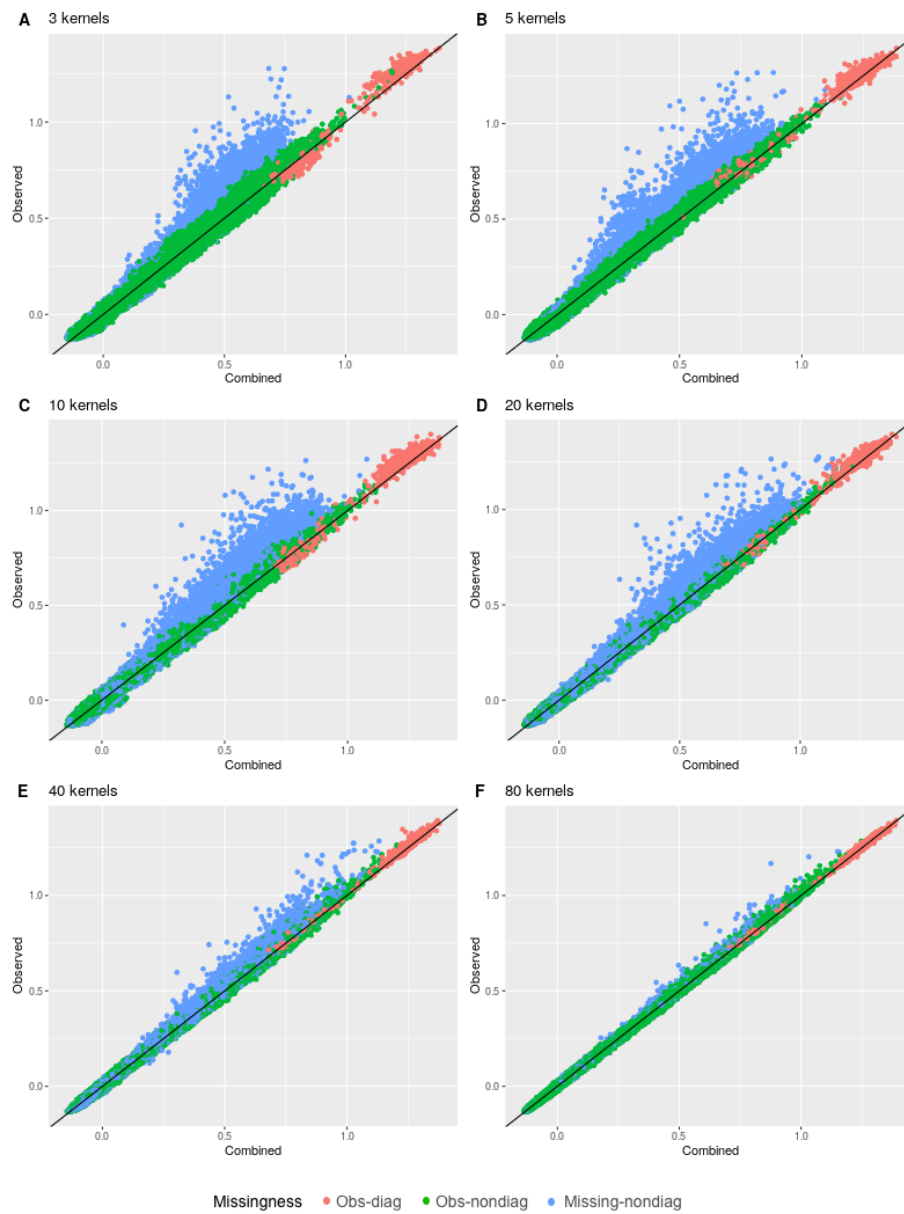


Fig. 8 Scatter plot of the lower triangular elements of the combined kernel against the kernel calculated from all available markers (Observed). As the number of incomplete data sets increases, both observed and unobserved parts of the relationship can be estimated more precisely.

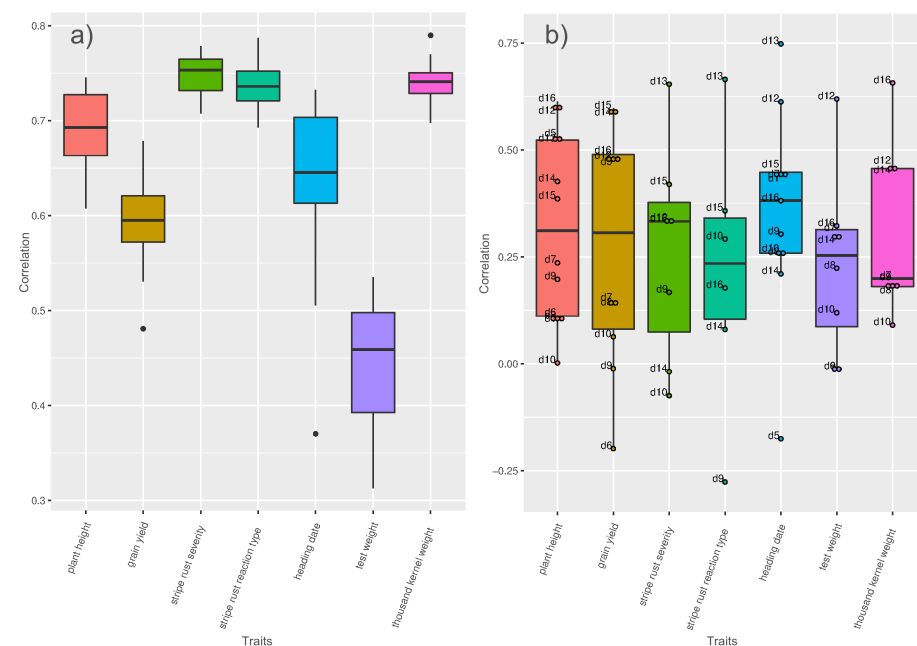
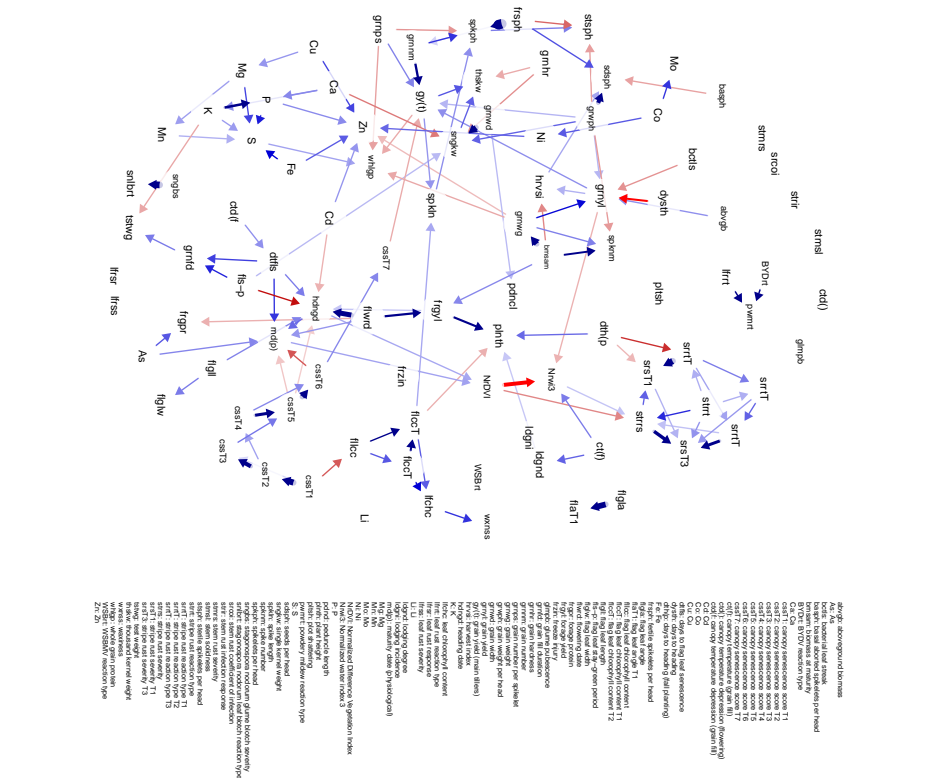


Fig. 9 Triticale data set: Cross-validation scenario 1 is shown in a. For each trait, the available genotypes were split into 10 random folds. The GEBVs for each fold were estimated from a mixed model (See Supplementary Section 5.4 for a description of this model) that was trained on the phenotypes available for the remaining genotypes. Cross-validation scenario 2 is shown in b. Genotypes in each genotypic data are the test and the remaining genotypes are training. In this case, each data that was predicted was also marked on the boxplots. For instance, for plant height, we can predict the phenotypes for the genotypes in d16 with high accuracy when we use the phenotypes of the remaining genotypes as training dataset; on the other hand, we have about zero accuracy when we try to estimate the genotypes in d10. The accuracy of the predictions under both scenarios were evaluated by calculating the correlations between the GEBVs and the observed trait values.

understand complex biological organisms. Issues and opportunities are beginning to emerge, like the promise of gathering phenotypical knowledge from totally independent datasets for meta-analyses.

To address the challenges of genomic and phenotypic data integration, we developed a simple and efficient approach for integrating data from multiple sources. This method can be used to combine information from multiple experiments across all levels of the biological hierarchy such as microarray, gene expression, microfluidics, and proteomics will help scientists to discover new information and to develop new approaches.

For example, Figure 7 shows that we can estimate the full genomic relationship matrix more precisely from 10 independent partially overlapping data sets of 200 genotypes and 2000 markers each than estimating from a data set (for the combined set of genotypes) that has 2000 fixed markers. Twenty independent genomic data sets of 200 genotypes and 2000 markers is as good as one genomic dataset with 5000 markers. When we compare it to the rest of the entries imputation is the least effective for estimating the unobserved parts of the genomic relationship



name	label	name	label	name	label	name	label
aboveground biomass	ab_g_bim	fertile spikelets per head	fsph	harvest index	hrvi	seeds per head	sdph
As	As	flag leaf angle	fla	heading date	hdn_dt	single kernel weight	sklw
bacterial leaf streak	bas_lfstr	flag leaf angle T1	flaT1	K	K	spike length	spkl
basal aborted spikelets per head	basn_abspk	flag leaf chlorophyll content	flcc	leaf chlorophyll content	lcc	spike number	spkn
biomass at maturity	bm_atm	flag leaf chlorophyll content T1	flccT1	leaf rust reaction type	lrrt	spikelets per head	spkh
Cu	Cu	flag leaf chlorophyll content T2	flccT2	leaf rust response	lfr	stem rust coefficient of infection	sroi
canopy senescence score T1	csT1	flag leaf length	fll	leaf rust severity	lfrs	stem rust infection response	srir
canopy senescence score T2	csT2	flag leaf stay-green period	flspg	Li	Li	stem rust severity	strs
canopy senescence score T3	csT3	flag leaf width	flw	lodging degree	ldg	stem solidness	stms
canopy senescence score T4	csT4	flowering date	flw_d	lodging incidence	ldgi	sterile spikelets per head	ssph
canopy senescence score T5	csT5	forage protein	frg_p	maturity date (physiological)	mtr_phy	stripe rust reaction type	srrt
canopy senescence score T6	csT6	forage yield	frg_y	Mg	Mg	stripe rust reaction type T1	srrtT1
canopy senescence score T7	csT7	frost injury	fri	Mn	Mn	stripe rust reaction type T2	srrtT2
canopy temperature (grain fill)	ctd_gf	glume pubescence	glmp	Mo	Mo	stripe rust reaction type T3	srrtT3
canopy temperature depression (flowering)	ctd_fl	grain fill duration	grfd	Ni	Ni	stripe rust severity	strs
canopy temperature depression (grain fill)	ctd_gf	grain hardness	grnh	Normalized Difference Vegetation Index	NDVI	stripe rust severity T1	srsT1
Cd	Cd	grain number	grn	Normalized water index 3	Nwi3	stripe rust severity T3	srsT3
Co	Co	grain number per spikelet	grnp	P	P	test weight	tsw
Cu	Cu	grain weight	grwt	P	P	thousand kernel weight	thkw
days to flag leaf senescence	dtfls	grain weight per head	grwh	plant height	plnh	waxiness	wxns
days to heading	d_t_h	grain width	grwd	plot shattering	plts	whole grain protein	wh_gp
days to heading (fall planting)	d_t_h_fp	grain yield	grny	powdery mildew reaction type	pmrt	WSDMV reaction type	WSDMV_rt
Fe	Fe	grain yield (main tillers)	grny_mt	S	S	Zn	Zn

Fig. 10 Triticale data set: Combining the phenotypic correlation matrices from 144 wheat data sets covering 95 traits and illustrating the relationships between traits using the DAG as a tool to explore the underlying relationships. Each node represents a trait and each edge represents a correlation between two traits. Blue edges indicate positive correlations, red edges indicate negative correlations, and the width and color of the edges correspond to the absolute value of the correlations: the higher the correlation, the thicker and more saturated is the edge.

matrix. This suggests that accounting for incomplete genetic relationships would be a more promising approach than estimating the genomic features by imputation and then calculating the genomic relationship matrix.

Figure 6 shows we can accurately estimate the unobserved relationships among the genotypes in two independent pedigree based relationship matrices by genotyping a small proportion of the genotypes in these data sets. For example, the mean correlation for the worst case setting (50 genotypes in each pedigree and 10 from each of the pedigree genotyped) was 0.72. This value increased all the way up to 0.94 for the best case (250 genotypes in each pedigree and 40 from each of the pedigree genotyped).

The selection in genomic selection is based on the genomically estimated breeding values (GEBVs). A common approach to obtaining GEBVs involves the use of a linear mixed model with a marker-based additive relationship matrix. If the phenotypic information corresponding to the genotypes in one or more of the component matrices are missing then the genotypic value estimates can be obtained using the available phenotypic information and the combined genomic information that links all the genotypes and the experiments.

Imputation has been the preferred method when dealing with incomplete and data sets [Browning, 2008, Browning and Browning, 2009, Howie et al., 2011, Druet et al., 2014, Erbe et al., 2016]. However, imputation can be inaccurate if the data is very heterogeneous [Van Buuren et al., 2011]. In these cases, as seen in examples above, the proposed approach which uses the relationships instead of the actual features seems to outperform imputation for inferring genomic relationships. Besides, the methods introduced in this article are useful even when imputation is not feasible. For example, two partially overlapping relationship matrices, one pedigree-based and the other can be combined to make inferences about the genetic similarities of genotypes in both of these data sets.

There are also limitations to our approach. In particular, when we combine data using relationship matrices original features are not imputed. Our method may not be the best option when inferences about genomic features are needed, such as in GWAS. We can address this issue by imputing the missing features using the combined relationship matrix for example using a k-nearest neighbor imputation [Hastie et al., 2001] or by kernel smoothing. Moreover, if the marker data in the independent genomic studies can be mapped to local genomic regions, then the combined relationship matrices can be obtained for these genomic regions separately and a kernel based model such as the ones in Yang et al. [2008], Akdemir and Jannink [2015] can be used for association testing. The nature of missingness in data will affect our algorithms performance. Inference based on approaches that ignore the missing data mechanisms are valid for missing completely at random (MCAR), missing at random (MAR) but probably not for not missing at random (NMAR) [Little and Rubin, 2002, Rubin, 1976].

4.1 Software and data availability

The software was written using C++ and R. The code for replicating some of the analysis can be requested from the corresponding author.

Acknowledgements

References

- Deniz Akdemir and Jean-Luc Jannink. Locally epistatic genomic relationship matrices for genomic association and prediction. *Genetics*, 199(3):857–871, 2015.
- Theodore W. Anderson. *An Introduction to Multivariate Statistical Analysis, 2nd Edition*. Wiley, sep 1984a. ISBN 0471889873. URL <https://www.xarg.org/ref/a/0471889873/>.
- TW Anderson. *An Introduction to Multivariate*. Wiley & Sons, 1984b.
- Bonnie Berger, Jian Peng, and Mona Singh. Computational solutions for omics data. *Nature reviews genetics*, 14(5):333–346, 2013.
- Matteo Bersanelli, Ettore Mosca, Daniel Remondini, Enrico Giampieri, Claudia Sala, Gastone Castellani, and Luciano Milanese. Methods for the integration of multi-omics data: mathematical aspects. *BMC bioinformatics*, 17(2):S15, 2016.
- Walter F Bodmer. Human genetics: the molecular challenge. In *Cold Spring Harbor symposia on quantitative biology*, volume 51, pages 1–13. Cold Spring Harbor Laboratory Press, 1986.
- Leo Breiman. Random forests. *Machine learning*, 45(1):5–32, 2001.
- Brian L Browning and Sharon R Browning. A unified approach to genotype imputation and haplotype-phase inference for large data sets of trios and unrelated individuals. *The American Journal of Human Genetics*, 84(2):210–223, 2009.
- Sharon R Browning. Missing data imputation and haplotype phase inference for genome-wide association studies. *Human genetics*, 124(5):439–450, 2008.
- Erhard Cramer. Conditional iterative proportional fitting for gaussian distributions. *Journal of multivariate analysis*, 65(2):261–276, 1998.
- Erhard Cramer. Probability measure with given marginals and conditionals: I-projections and conditional iterative proportional fitting. *Statistics & Risk Modeling*, 18(3):311–330, 2000.
- José Crossa, Paulino Pérez-Rodríguez, Jaime Cuevas, Osval Montesinos-López, Diego Jarquín, Gustavo de los Campos, Juan Burgueño, Juan M González-Camacho, Sergio Pérez-Elizalde, Yoseph Beyene, et al. Genomic selection in plant breeding: methods, models, and perspectives. *Trends in plant science*, 22(11):961–975, 2017.
- Gustavo de los Campos, John M Hickey, Ricardo Pong-Wong, Hans D Daetwyler, and Mario PL Calus. Whole-genome regression and prediction methods applied to plant and animal breeding. *Genetics*, 193(2):327–345, 2013.
- A.P. Dempster, N.M. Laird, and D.B. Rubin. Maximum likelihood from incomplete data via the em algorithm. *Journal of the Royal Statistical Society. Series B (Methodological)*, pages 1–38, 1977.
- Arthur P Dempster, Donald B Rubin, and Robert K Tsutakawa. Estimation in covariance components models. *Journal of the American Statistical Association*, 76(374):341–353, 1981.
- Zeratsion Abera Desta and Rodomiro Ortiz. Genomic selection: genome-wide prediction in plant improvement. *Trends in plant science*, 19(9):592–601, 2014.
- Tom Druet, IM Macleod, and BJ Hayes. Toward genomic prediction from whole-genome sequence data: impact of sequencing design on genotype imputation and accuracy of predictions. *Heredity*, 112(1):39, 2014.
- Jeffrey B Endelman. Ridge regression and other kernels for genomic selection with r package rrblup. *The Plant Genome*, 4(3):250–255, 2011.

- Jeffrey B Endelman, Cari A Schmitz Carley, Paul C Bethke, Joseph J Coombs, Mark E Clough, Washington L da Silva, Walter S De Jong, David S Douches, Curtis M Frederick, Kathleen G Haynes, et al. Genetic variance partitioning and genome-wide prediction with allele dosage information in autotetraploid potato. *Genetics*, 209(1):77–87, 2018.
- Sacha Epskamp, Angélique O. J. Cramer, Lourens J. Waldorp, Verena D. Schmittmann, and Denny Borsboom. qgraph: Network visualizations of relationships in psychometric data. *Journal of Statistical Software*, 48(4):1–18, 2012. URL <http://www.jstatsoft.org/v48/i04/>.
- Malena Erbe, Mirjam Frischknecht, Hubert Pausch, Reiner Emmerling, TH Meuwissen, Birgit Gredler, Beat Bapst, I Consortium, KU Götzt, and H Simianer. 0409 genomic prediction using imputed sequence data in dairy and dual purpose breeds. *Journal of Animal Science*, 94(suppl.5):198–199, 2016.
- Cedric Gondro, Julius Van der Werf, and Ben J Hayes. *Genome-wide association studies and genomic prediction*. Springer, 2013.
- Serap Gonen, Valentin Wimmer, R Chris Gaynor, Ed Byrne, Gregor Gorjanc, and John M Hickey. A heuristic method for fast and accurate phasing and imputation of single-nucleotide polymorphism data in bi-parental plant populations. *Theoretical and applied genetics*, 131(11):2345–2357, 2018.
- A.K. Gupta and D.K. Nagar. *Matrix Variate Distributions*. Chapman and Hall/CRC Monographs and Surveys in Pure and Applied Mathematics. Chapman and Hall, 2000.
- T. Hastie, R. Tibshirani, B. Narasimhan, G. Chu, T. Hastie, R. Tibshirani, B. Narasimhan, and G. Chu. impute: Imputation for microarray data. *Bioinformatics*, 17(6):520–525, 2001.
- Trevor Hastie and Rahul Mazumder. *softImpute: Matrix Completion via Iterative Soft-Thresholded SVD*, 2015. URL <https://CRAN.R-project.org/package=softImpute>. R package version 1.4.
- Elliot L Heffner, Aaron J Lorenz, Jean-Luc Jannink, and Mark E Sorrells. Plant breeding with genomic selection: gain per unit time and cost. *Crop science*, 50(5):1681–1690, 2010.
- Elliot L Heffner, Jean-Luc Jannink, Hiroyoshi Iwata, Edward Souza, and Mark E Sorrells. Genomic selection accuracy for grain quality traits in biparental wheat populations. *Crop Science*, 51(6):2597–2606, 2011.
- William G Hill and Trudy FC Mackay. Ds falconer and introduction to quantitative genetics. *Genetics*, 167(4):1529–1536, 2004.
- Bryan Howie, Jonathan Marchini, and Matthew Stephens. Genotype imputation with thousands of genomes. *G3: Genes, Genomes, Genetics*, 1(6):457–470, 2011.
- Philomin Juliana, Ravi P Singh, Jesse Poland, Suchismita Mondal, José Crossa, Osva A Montesinos-López, Susanne Dreisigacker, Paulino Pérez-Rodríguez, Julio Huerta-Espino, Leonardo Crespo-Herrera, et al. Prospects and challenges of applied genomic selection—a new paradigm in breeding for grain yield in bread wheat. *The plant genome*, 11(3), 2018.
- Tonu Kollo and Dietrich von Rosen. *Advanced multivariate statistics with matrices*, volume 579. Springer Science & Business Media, 2006.
- Andres Legarra, I Aguilar, and I Misztal. A relationship matrix including full pedigree and genomic information. *Journal of dairy science*, 92(9):4656–4663, 2009.

- RJA Little and DB Rubin. Statistical analysis with missing data. wiley. *New York*, 2002.
- Elaine R Mardis. The impact of next-generation sequencing technology on genetics. *Trends in genetics*, 24(3):133–141, 2008a.
- Elaine R Mardis. Next-generation dna sequencing methods. *Annu. Rev. Genomics Hum. Genet.*, 9:387–402, 2008b.
- T. H. E. Meuwissen, B. J. Hayes, and M. E. Goddard. Prediction of total genetic value using genome-wide dense marker maps. *Genetics*, 157(4):1819–1829, 2001.
- EL Nicolazzi, S Biffani, and G Jansen. Imputing genotypes using pedimpute fast algorithm combining pedigree and population information. *Journal of dairy science*, 96(4):2649–2653, 2013.
- Rodrigo Rampazo Amadeu, Catherine Cellon, James W Olmstead, Antonio Augusto Franco Garcia, and Marcio FR Resende Jr. Aghmatrix: R package to construct relationship matrices for autotetraploid and diploid species: A blueberry example. *The Plant Genome*, 9(3):1–10, 2016.
- Neil Risch and Kathleen Merikangas. The future of genetic studies of complex human diseases. *Science*, 273(5281):1516–1517, 1996.
- Donald B Rubin. Inference and missing data. *Biometrika*, 63(3):581–592, 1976.
- Jessica E Rutkoski, Jesse Poland, Jean-Luc Jannink, and Mark E Sorrells. Imputation of unordered markers and the impact on genomic selection accuracy. *G3: Genes, Genomes, Genetics*, 3(3):427–439, 2013.
- B. Schölkopf and A. Smola. *Learning with kernels*. MIT Press, Cambridge, MA, 2005.
- Fiona M Shrive, Heather Stuart, Hude Quan, and William A Ghali. Dealing with missing data in a multi-question depression scale: a comparison of imputation methods. *BMC medical research methodology*, 6(1):57, 2006.
- Stef Van Buuren et al. Multiple imputation of multilevel data. *Handbook of advanced multilevel analysis*, 10:173–196, 2011.
- Paul M VanRaden, Chuanyu Sun, and Jeffrey R O’Connell. Fast imputation using medium or low-coverage sequence data. *BMC genetics*, 16(1):82, 2015.
- PM VanRaden. Efficient methods to compute genomic predictions. *Journal of dairy science*, 91(11):4414–4423, 2008.
- Peter M Visscher, Naomi R Wray, Qian Zhang, Pamela Sklar, Mark I McCarthy, Matthew A Brown, and Jian Yang. 10 years of gwas discovery: biology, function, and translation. *The American Journal of Human Genetics*, 101(1):5–22, 2017.
- Hsin-Chou Yang, Hsin-Yi Hsieh, and Cathy SJ Fann. Kernel-based association test. *Genetics*, 179(2):1057–1068, 2008.

Supplementary Materials: Adventures in Multi-Omics I: Combining heterogeneous data sets via relationships

5 Supplementary Methods

5.1 Wishart EM-Algorithm

The Wishart EM-Algorithm maximizes the likelihood function for a random sample of incomplete observations from a Wishart distribution with fixed degrees of freedom since it is an EM-Algorithm [Dempster et al., 1977, 1981]. To the best of our knowledge, this is the first study that derives the EM-Algorithm for the following case. Let $G_{a_1}, G_{a_2}, \dots, G_{a_m}$ be independent and partial realizations from a Wishart distribution with a known degrees of freedom $\nu > n$ and covariance parameter $\Psi = \Sigma/\nu$. Expectation of each G_a is therefore equal to Σ_a .

The likelihood function for the observed data can be written as

$$\begin{aligned} L(\Psi|\nu, G_{a_1}, G_{a_2}, \dots, G_{a_m}) &= \prod_{i=1}^m W(G_{a_i}|\nu, \Sigma_{a_i}) \\ &= \prod_{i=1}^m \frac{|G_{a_i}|^{(\nu-k_i-1)/2} \exp(-\frac{1}{2}tr(\Psi^{-1}G_{a_i}))}{\left(2^{\nu k_i/2} \pi^{k_i(k_i-1)/4} \prod_{j=1}^{k_i} \Gamma(\frac{\nu+1-j}{2})\right) |\Psi_{a_i}|^{\nu/2}} \end{aligned}$$

The log-likelihood function with the constant terms combined in c is given by

$$l(\Psi|\nu, G_{a_1 a_1}, G_{a_2 a_2}, \dots, G_{a_m a_m}) = c - \frac{1}{2} \sum_{i=1}^m \left[tr(\Psi_{a_i}^{-1} G_{a_i}) + \nu \log |\Psi_{a_i}| \right].$$

Complementing each of the observed data with the missing data components $G_B = (G_{ab}, G_b)$, we can write the log-likelihood for the complete data up to a constant term as follows:

$$\begin{aligned} \ell^c(\Psi|\nu, G_{a_1}, G_{a_2}, \dots, G_{a_m}, G_{B_1}, G_{B_2}, \dots, G_{B_m}) &= \frac{\nu - n - 1}{2} \left(\sum_{i=1}^m \log |G_{a_i}| \right) \\ &+ \sum_{i=1}^m |G_{b_i} - G'_{ab_i} G_{a_i}^{-1} G_{ab_i}| \\ &\quad - \frac{\nu}{2} \left(\sum_{i=1}^m \log |\Psi_{a_i}| \right) \\ &+ \sum_{i=1}^m \log |\Psi_{b_i} - \Psi'_{ab_i} \Psi_{a_i}^{-1} \Psi_{ab_i}| \\ &\quad - \frac{1}{2} tr(\Psi^{-1} \sum_{i=1}^m G_i) \end{aligned}$$

The expectation step of the EM-Algorithm involves calculating the expectation of the complete data log-likelihood conditional on observed data and the value of Ψ at iteration t which we denote by $\Psi^{(t)}$.

$$\begin{aligned} E \left[\ell^c(\Psi | \nu, G_{a_1}, G_{a_2}, \dots, G_{a_m}, G_{B_1}, G_{B_2}, \dots, G_{B_m}) | G_{a_1}, G_{a_2}, \dots, G_{a_m}, \Psi^{(t)} \right] \\ = \frac{v-n-1}{2} \left(\sum_{i=1}^m \log |G_{a_i}| \right) \\ + \sum_{i=1}^m |\Psi_{b_i}^{(t)} - \Psi^{(t)'}_{ab_i} \Psi^{(t)-1}_a \Psi_{ab_i}^{(t)}| \\ - \frac{vm}{2} \log |\Psi| \\ - \frac{1}{2} \text{tr}(\Psi^{-1} \sum_{i=1}^m E [G_i | G_{a_i}, \Psi^{(t)}]) \end{aligned}$$

The maximization step of the EM algorithm which updates $\Psi^{(t)}$ to $\Psi^{(t+1)}$ by finding Ψ that maximizes the expected complete data log-likelihood. (Using [Anderson, 1984b, Lemma 3.3.2]) The solution is given by:

$$\Psi^{(t+1)} = \frac{\sum_{i=1}^m E [G_i | G_{a_i}, \Psi^{(t)}]}{vm}.$$

We need to calculate $E [G_i | G_{a_i}, \Psi^{(t)}]$ for each i . G is partitioned as

$$\begin{bmatrix} G_a & G_{ab} \\ G'_{ab} & G_b \end{bmatrix}.$$

We assume a similar partitioning for Ψ .

Firstly, $E [G_a | G_{a_i}, \Psi^{(t)}]$ is G_a . Secondly, $G_{ab} | G_{a_i}, \Psi^{(t)}$ has a matrix-variate normal distribution with mean $G_a \Psi_a^{(t)-1} \Psi_{ab}^{(t)}$ (the covariance of the vectorized form is given by $G_a \otimes (\Psi_b^{(t)} - \Psi^{(t)'}_{ab} \Psi_a^{(t)-1} \Psi_{ab}^{(t)})$).

To calculate the expectation of G_b , note that we can write this term as $G_b = (G_b - G'_{ab} G_a^{-1} G_{ab}) + G'_{ab} G_a^{-1} G_{ab}$. The distribution of the first term is independent of G_a and G_{ab} and is a Wishart distribution with degrees of freedom $\nu - n_a$ and covariance parameter $\Psi_b^{(t)} - \Psi^{(t)'}_{ab} \Psi_a^{(t)-1} \Psi_{ab}^{(t)}$. The second term is an inner product $(G_a^{-\frac{1}{2}} G_{ab})' (G_a^{-\frac{1}{2}} G_{ab})$. The distribution of $G_a^{-\frac{1}{2}} G_{ab}$ is a matrix-variate normal distribution with mean $G_a^{\frac{1}{2}} \Psi_a^{(t)-1} \Psi_{ab}^{(t)}$ and covariance is given by $\Psi_b^{(t)} - \Psi^{(t)'}_{ab} \Psi_a^{(t)-1} \Psi_{ab}^{(t)}$, I_{n_a} for the columns and rows correspondingly. The expectation of this inner-product is $\Psi^{(t)'}_{ab} \Psi_a^{(t)-1} G_a + n_a (\Psi_b^{(t)} - \Psi^{(t)'}_{ab} \Psi_a^{(t)-1} \Psi_{ab}^{(t)})$. Therefore, the expected value of G_b given $G_a, \Psi^{(t)}$ is $\Psi^{(t)'}_{ab} \Psi_a^{(t)-1} G_a \Psi_a^{(t)-1} \Psi_{ab}^{(t)} + n_a (\Psi_b^{(t)} - \Psi^{(t)'}_{ab} \Psi_a^{(t)-1} \Psi_{ab}^{(t)}) + (\nu - n_a) (\Psi_b^{(t)} - \Psi^{(t)'}_{ab} \Psi_a^{(t)-1} \Psi_{ab}^{(t)}) = \nu (\Psi_b^{(t)} - \Psi^{(t)'}_{ab} \Psi_a^{(t)-1} \Psi_{ab}^{(t)}) + \Psi^{(t)'}_{ab} \Psi_a^{(t)-1} G_a \Psi_a^{(t)-1} \Psi_{ab}^{(t)}$. This leads to the update equation:

$$\Psi^{(t+1)} = \frac{1}{\nu m} \sum_{a \in A} P_a \begin{bmatrix} G_{aa} & G_{aa} (B_{b|a}^{(t)})' \\ B_{b|a}^{(t)} G_{aa} & \nu \Psi_{bb|a}^{(t)} + B_{b|a}^{(t)} G_{aa} (B_{b|a}^{(t)})' \end{bmatrix} P'_a \quad (S1)$$

where $B_{b|a}^{(t)} = \Psi_{ab}^{(t)}(\Psi_{aa}^{(t)})^{-1}$, $\Psi_{bb|a}^{(t)} = \Psi_{bb}^{(t)} - \Psi_{ab}^{(t)}(\Psi_{aa}^{(t)})^{-1}\Psi_{ba}^{(t)}$, a is the set of genotypes in the given partial genomic relationship matrix and b is the set difference of K and a . The matrices P_a are permutation matrices that put each matrix in the sum in the same order. The initial value, $\Sigma^{(0)}$ is usually assumed to be an identity matrix of dimension n .

During the steps of the Wishart EM-Algorithm we might encounter a matrix Ψ which is not positive definite. There are two strategies to deal with this case: 1) allow Ψ to be non definite but replace it with a near positive definite matrix after last iteration, 2) force Ψ to be positive definite at each iteration by replacing it with a near positive definite matrix. We have used the second approach in our implementations.

Asymptotic standard errors

Once the maximizer of $l(\Psi)$, $\hat{\Psi} = \Psi^\infty$, has been found, the asymptotic standard errors can be calculated from the information matrix of Ψ evaluated at $\hat{\Psi}$. Equivalently, the information matrix can be obtained from hessian of the expected value of the complete data likelihood given $\hat{\Psi}$ and $G_{a_1}, G_{a_2}, \dots, G_{a_m}$ evaluated at $\hat{\Psi}$. Following the latter route, and letting

$$\hat{H}_a = P_a \begin{bmatrix} G_{aa} & G_{aa}(B_{b|a}^{(\infty)})' \\ B_{b|a}^{(\infty)} G_{aa} \nu \Psi_{bb|a}^{(\infty)} + B_{b|a}^{(\infty)} G_{aa} (B_{b|a}^{(\infty)})' \end{bmatrix} P_a'$$

the information matrix for Ψ is obtained as

$$\{I(\Psi)\}_{jk, lh} = \{-E(\frac{\partial^2 l(\Psi)}{\partial \psi_{jk} \partial \psi_{lh}} | \Psi = \hat{\Psi})\}_{jk, lh} = \frac{\nu}{2} \sum_{a \in A} \left[tr(\hat{H}_a^{-1} \frac{\partial \Psi}{\partial \psi_{jk}} \hat{H}_a^{-1} \frac{\partial \Psi}{\partial \psi_{lh}}) \right]$$

It is important to notice that the estimator of $\Sigma = \nu\Psi$ does not depend on the value of nu , but the asymptotic sampling covariance of this estimator does.

5.2 Some Properties of Matrix Normal and Wishart Distribution

The following results and their derivations are given in classic multivariate statistics textbooks such as [Anderson, 1984a] and [Gupta and Nagar, 2000, Kollo and von Rosen, 2006] and are used in the derivation of the Wishart EM-Algorithm.

- [Kollo and von Rosen, 2006, Theorem 2.2.9] Let $X \sim N_{p,n}(M, \Sigma, \Psi)$. Then, $E[XAX'] = tr(\Psi A)\Sigma + MAM'$.
- [Kollo and von Rosen, 2006, Theorem 2.4.12.] Let $G \sim W_n(\nu, \Psi)$ with Ψ and $\nu > n$.
- Density

$$p(G) = \mathcal{W}_\nu(G|\Psi) = \frac{|G|^{(\nu-k-1)/2} \exp(-\frac{1}{2}tr(\Psi^{-1}G))}{2^{\nu k/2} \pi^{k(k-1)/4} \prod_{i=1}^k \Gamma(\frac{\nu+1-i}{2}) |\Psi|^{nu/2}}$$

- $E(G) = \nu\Psi$
- $G_{1|2}$ is independent of (G_{12}, G_{22}) ;
- $G_{22} \sim W_q(\nu, \Psi_{22})$;
- The conditional distribution of G_{12} given G_{22} is multivariate Gaussian $N_{(n-q) \times q}(\Psi_{12}\Psi_{22}^{-1}G_{22}, A)$ where $A_{ij, kl} = Cov(G_{ij}, G_{kl}|G_{22}) = \Psi_{ik}^{1|2} G_{jl}$.

5.3 Genomic features, distances and kernel matrices

Let M be the $n \times m$ matrix of biallelic marker allele dosages for n diploid genotypes and m markers, and let $n < m$. The vector of estimates of allele probabilities is given by $\mathbf{p}'_m = (\mathbf{1}'_n M)/(2n)$. Let $X_m = (M - 2\mathbf{1}_n \mathbf{p}'_m)/\sqrt{c_m}$ be the feature matrix where $c_m = 2 \sum_{i=1}^m p_{m_i}(1 - p_{m_i})$. An additive relationship matrix can be written as $= X_m X'_m$ [VanRaden, 2008]. This matrix is singular.

A similar relationship matrix that is nonsingular can be obtained by changing the centering and scaling of the allele dosages matrix. Let $\mathbf{p}_n = (\mathbf{1}'_m M')/(2m)$. Let $X = (M - 2\mathbf{p}_n \mathbf{1}'_m)/\sqrt{c} = M(I_n - \mathbf{1}_n \mathbf{1}'_n/n)/\sqrt{c}$ be the feature matrix where $c = \frac{1}{n} \sum_{i=1}^n \sum_{j=1}^m X_{ij}^2$. X is the row centered feature matrix scaled by the mean square root of total average heterozygosity for the genotypes. We also use the notation $G_A(X) = X X'$ and note that $G_A(X)$ can be calculated from by covariance matrix for the genotypes of the marker allele dosages matrix M by dividing it by the mean of its diagonal elements (abusing notation, this can be expressed as $G_A(X) = \text{cov}(M')/\text{mean}(\text{diag}(\text{cov}(M')))$). This matrix is non-singular whenever the number of independent features in the data are larger than the sample size. The mean of the diagonals of this relationship matrix is one. More importantly, the same formulation applies to all types of genomic features. For instance, we can use the same formulation for marker data with higher ploidy levels, or with other forms of genomic data such as the expression data.

For each pair of genotypes $((i, j) : i, j \in (1, 2, \dots, n))$ in M , the squared Euclidean distance using the corresponding a feature matrix $X = (\mathbf{x}_1, \mathbf{x}_2, \dots, \mathbf{x}_n)'$ can be written as

$$d_{ij} = (\mathbf{x}_i - \mathbf{x}_j)'(\mathbf{x}_i - \mathbf{x}_j) = \mathbf{x}'_i \mathbf{x}_i + \mathbf{x}'_j \mathbf{x}_j - 2\mathbf{x}'_i \mathbf{x}_j = (G_A)_{ii} + (G_A)_{jj} - 2(G_A)_{ij}.$$

The squared distance matrix is defined by $D(X) = (d_{ij})$ and can be calculated from the additive relationship matrix $G_A(X) = X X'$ as

$$\begin{aligned} D(X) &= \mathbf{1}_n \text{diag}(X X')' + \text{diag}(X X') \mathbf{1}'_n - 2X X' \\ &= \mathbf{1}_n \text{diag}(G_A)' + \text{diag}(G_A) \mathbf{1}'_n - 2G_A \end{aligned}$$

Moreover, since $\mathbf{1}' X = \mathbf{0}$ and $(I - \frac{\mathbf{1}\mathbf{1}'}{n})\mathbf{1} = \mathbf{1} - \mathbf{1} \frac{\mathbf{1}'\mathbf{1}}{n} = \mathbf{1} - \mathbf{1} \frac{n}{n} = \mathbf{0}$, we have

$$\begin{aligned} (I - \frac{\mathbf{1}\mathbf{1}'}{n})D(X)(I - \frac{\mathbf{1}\mathbf{1}'}{n}) &= (I - \frac{\mathbf{1}\mathbf{1}'}{n})(\mathbf{1}_n \text{diag}(G_A)' + \text{diag}(G_A) \mathbf{1}'_n - 2G_A)(I - \frac{\mathbf{1}\mathbf{1}'}{n}) \\ &= -2X X' = 2G_A. \end{aligned}$$

Therefore, given $D(X)$ and letting $P = (I - \frac{\mathbf{1}\mathbf{1}'}{n})$ the additive relationship matrix can also be calculated by

$$G_A = -\frac{1}{2} P D P.$$

The genomic relationship matrices need not be additive. RKHS regression extends additive relationship based SPMMs by allowing a wide variety of kernel matrices, not necessarily additive in the input variables, calculated using a variety of kernel functions. A kernel function, $k(\cdot, \cdot)$ maps a pair of input points \mathbf{x} and \mathbf{x}' into

real numbers. It is by definition symmetric ($k(\mathbf{x}, \mathbf{x}') = k(\mathbf{x}', \mathbf{x})$) and non-negative. Given the inputs for the n genotypes we can compute a kernel matrix G whose entries are $G_{ij} = k(\mathbf{x}_i, \mathbf{x}_j)$. The linear kernel function is given by $k(\mathbf{x}; \mathbf{y}) = \mathbf{x}'\mathbf{y}$. The polynomial kernel function is given by $k(\mathbf{x}; \mathbf{y}) = (\mathbf{x}'\mathbf{y} + c)^d$ for c and $d \in \mathbb{R}$. Finally, the Gaussian kernel function is given by $k(\mathbf{x}; \mathbf{y}) = \exp(-h(\mathbf{x}' - \mathbf{y}')(\mathbf{x}' - \mathbf{y}'))$ where $h > 0$. The common choices for kernel functions are the linear, polynomial, Gaussian kernel functions, though many other options are available [Schölkopf and Smola, 2005, Endelman, 2011].

The relationship between the Euclidean distance matrix and the corresponding Gaussian kernel is given by

$$G_G^h(X) = \exp(-h * D(X))$$

and

$$D(X) = -\frac{\log(G_G^h(X))}{h}.$$

An important advantage of using similarity or distance matrices over the original features is that similarity of distance matrices can be calculated for variables of different type (categorical, rank, or interval-scale data). The relationship of the feature matrix, and the additive kernel and Euclidean distance allows us to generalize the additive relationship matrix to general genomic data (not necessarily marker allele dosages).

5.4 Mixed models and genomic relationship matrices

Let's start by describing how we can use a single combined genomic data. The discussion below will be biased towards a discussion variance components / mixed modeling approach since this has a special place in quantitative genetics. Mixed models have been used as a formal way of partitioning the variability observed in traits into heritable and environmental components, it is also useful in controlling for population structure and relatedness for genome-wide association studies (GWAS). However, some of the methods that are proposed can be used in other forms of statistical analysis, for example, for descriptive purposes or in general statistical learning.

In a mixed model, genetic information in the form of a pedigree or marker allele frequencies can be used in the form of an additive genetic similarity matrix that describes the similarity based on additive genetic effects (GBLUP). For the $n \times 1$ response vector \mathbf{y} , the GBLUP model can be expressed as

$$\mathbf{y} = X\beta + Z\mathbf{u} + \mathbf{e} \tag{S2}$$

where X is the $n \times p$ design matrix for the fixed effects, β is a $p \times 1$ vector of fixed effect coefficients, Z is the $n \times q$ design matrix for the random effects; the vector random effects $(\mathbf{u}', \mathbf{e}')'$ is assumed to follow a multivariate normal (MVN) distribution with mean $\mathbf{0}$ and covariance

$$\begin{pmatrix} \sigma_g^2 G & \mathbf{0} \\ \mathbf{0} & \sigma_e^2 I_n \end{pmatrix} \tag{S3}$$

where G is the $q \times q$ additive genetic similarity matrix. In this model, the labels of the genotypes (that are listed in the rows and columns of the relationship matrix G) define a factor variable with levels equal to the labels. The matrix Z is the design matrix that links the observed response in the experiment to these levels. The model (S2) is equivalent to a MM in which the additive marker effects are estimated via the following model (rr-BLUP):

$$\mathbf{y} = X\boldsymbol{\beta} + ZM\mathbf{u} + \mathbf{e} \quad (\text{S4})$$

where X is the $n \times p$ design matrix for the fixed effects, $\boldsymbol{\beta}$ is a $p \times 1$ vector of fixed effect coefficients, Z is the $n \times q$ design matrix for the random effects M is $q \times m$ marker allele frequency centered incidence matrix; $(\mathbf{u}', \mathbf{e}')'$ follows a MVN distribution with mean $\mathbf{0}$ and covariance

$$\begin{pmatrix} \sigma_u^2 I_m & \mathbf{0} \\ \mathbf{0} & \sigma_e^2 I_n \end{pmatrix}.$$

Note that the scale of the genomic relationship matrix is irrelevant for genomic prediction or for family structure correction in mixed model-based association studies. However, this quantity is important for the calculation of narrow-sense heritability. In this case, setting the average of the diagonals of the relationship makes it, in a way, compatible with the broad sense heritability calculations based on an identity relationship matrix for genotypes that already has a mean of its diagonal elements equal to one. In addition, the standard formulations of the marker-based additive matrix models used in the literature can be generalized to incorporate more complex genetic and environmental covariates.

6 Supplementary Examples

6.1 Experiments with simulated data

Supplementary Example 1- Simulation study: Inferring the combined covariance matrix from its parts

To establish that a combined relationship can be inferred from realizations of its parts, we have conducted the following simulation study: In each round of the simulation, the true parameter value of the genomic relationship matrix was generated as $\Sigma = \text{diag}(r_1, r_2, \dots, r_{N_{Total}}) + .3 * \mathbf{1}_{N_{Total} \times N_{Total}}$ where r_i were independently generated as $1 + .7 * u_i$ with u_i a realization from the uniform distribution over $(0, 1)$. Σ was then adjusted by dividing it with the mean value of its diagonal elements. This parameter was taken as the covariance parameter of a Wishart distribution with degrees of freedom 300 and N_{kernel} samples from this distribution are generated. After that, each of the realized relationship matrices was made partial by leaving a random sample of 10 to 40 (this number was also selected from the discrete uniform distribution for integers 10 to 40) genotypes in it. These partial kernel matrices were combined using the Wishart EM-Algorithm iterated for 50 rounds (each round cycles through the partial relationship matrices in random order). The resultant combined relationship matrix $\hat{\Sigma}$ was compared

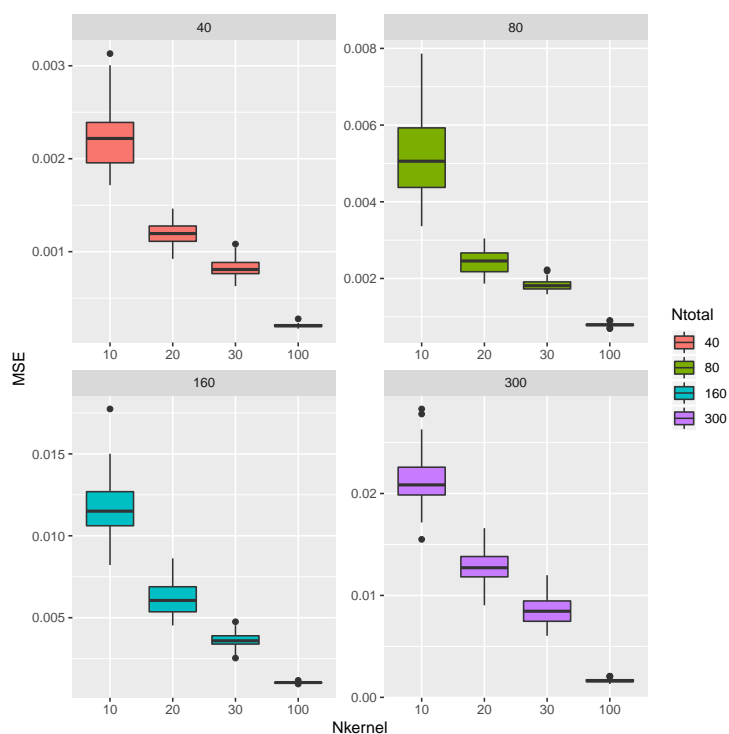


Fig. S1 Example 1 - MSE's for estimating correlation parameters based on partial samples for $N_{Total} \in \{40, 80, 150, 300\}$ (number of variables in the covariance matrix) and $N_{kernel} \in \{40, 80, 150, 300\}$ (number of incomplete covariance matrix samples). Each incomplete covariance matrix was had a random size between 10 to 40. The MSE's are calculated over 10 replications of the experiment.

with the corresponding parts of the parameter Σ^3 by calculating the mean squared error between the upper diagonal elements of these matrices. This experiment was replicated 10 times for each value of $N_{Total} \in \{40, 80, 150, 300\}$ and $N_{kernel} \in \{40, 80, 150, 300\}$.

The results of this simulation study are summarized in Figure S1. For each covariance size, the MSE's decreased as the number of incomplete samples increased. On the other hand, as the size of the covariance matrix increased the MSEs increased.

Supplementary Example 2- Simulation study: Likelihood Convergence

The Wishart EM-Algorithm maximizes the likelihood function for a random sample of incomplete observations from a Wishart distribution. The derivation of this feature is given in the Supplementary. In this example, we explore the convergence of the algorithm for several instances starting from several different initial estimates.

³ In certain instances, the union of the genotypes in the parts did not recover all of the N_{Total} genotypes, therefore this calculation was based on the recovered part of the full genomic relationship matrix

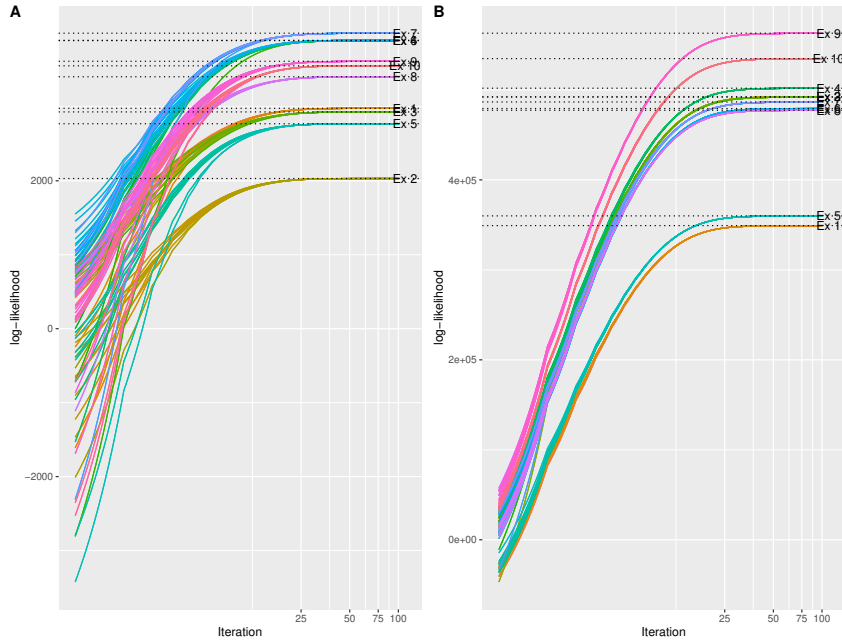


Fig. S2 Example 2 - Convergence of log-likelihood function: Each color represents a different experiment. In each experiment, a sample of incomplete covariance matrices from a Wishart distribution were combined using the Wishart EM-Algorithm starting from 10 different slightly different random initial estimates. n , the total number of genotypes in the assumed relationship matrix was taken to be 100 (A) or 1000 (B).

The example is composed of 10 experiments each of which starts with a slightly different assumed Wishart covariance parameter⁴. For each true assumed covariance matrix, we have generated 10 partial samples including between n_{min} and n_{max} genotypes (random at discrete uniform from n_{min} to n_{max}) each using the Wishart distribution. n , the total number of genotypes in the assumed relationship matrix was taken to be 100 or 1000. Corresponding to this two matrix sizes the n_{min} and n_{max} are taken as 10 and 25 or 100 and 250. These 10 matrices are combined using the Wishart EM-Algorithm 10 different times each times using a slightly different initial estimate of the covariance parameter⁵. We record the path of the log-likelihood function for all these examples.

At each instance of the parameter and a particular sample, the likelihood functions converged to the same point (See Figure S2). We have not observed any abnormalities in convergence according to these graphs.

Heatmap for 95 wheat traits

Phenotypic network for 186 traits based on phenotypic correlations (Wheat, Barley, and Oat Phenotypic Trials from Triticale Toolbox)

⁴ $\Sigma = \text{diag}(\mathbf{b} + 1) + .2\mathbf{1}_{n \times n}$ where \mathbf{b}_i for $i = 1, 2, \dots, n$ are i.i.d. uniform between 0 and 1.

⁵ $\Sigma_0 = \text{diag}(.5\mathbf{b} + 1) + .3 * \mathbf{b}_0 \mathbf{1}_{n \times n}$ where \mathbf{b}_i for $i = 0, 2, \dots, n$ are i.i.d. uniform between 0 and 1.

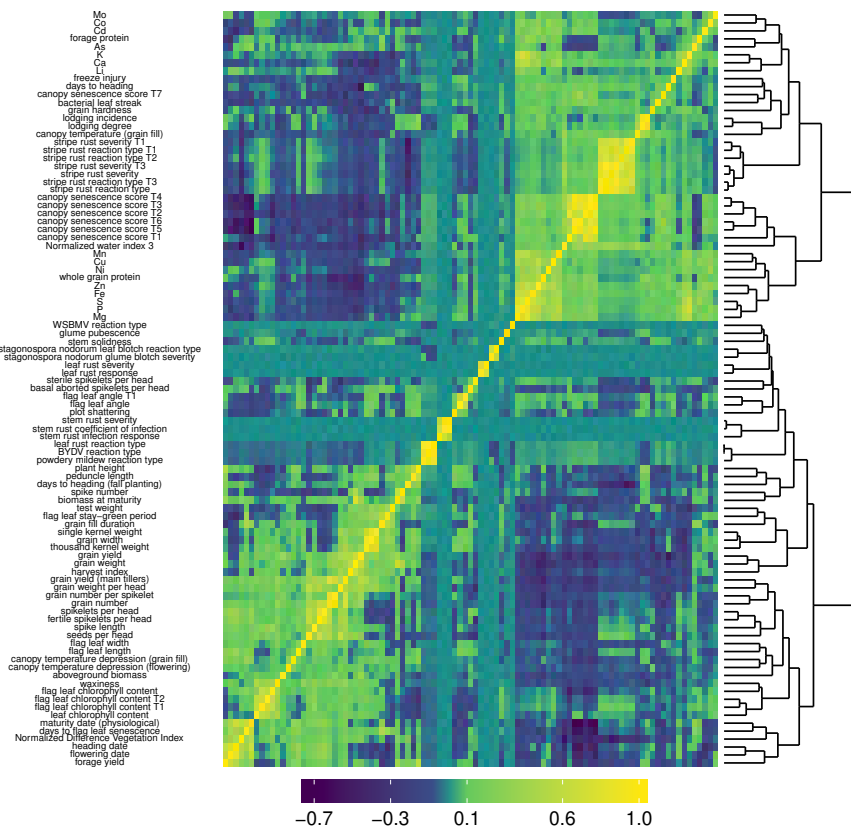
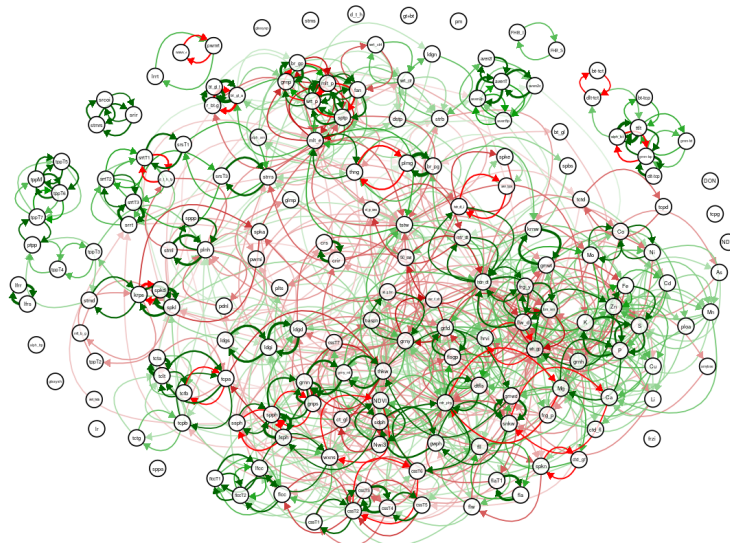


Fig. S3 Triticale data set: Combining the phenotypic correlation matrices from 144 wheat data sets covering 95 traits. Clustered heatmap of Pearson correlation coefficients provides a global overview of phenotypic correlation across wheat traits. Yellow denotes high correlation, dark green high anti-correlation.

6.2 Supplementary Figures



name	label	name	label	name	label	name	label
50 seed weight	50_swr	Cd	Cd	grain fill duration	gfd	Normalized Difference Vegetation Index	NDVI
aboveground biomass	abg_biom	Co	Co	grain hardness	grah	Normalized water index 3	NWI3
alpha amylase	alpha_am	crowm rust infection response	crr	grain number	gran	P	P
alpha-tocopherol	alpha_tocp	crowm rust severity	crs	grain number per spikelet	gnps	peduncle length	plnlg
alpha-tocotrienol	alpha_tocet	Cu	Cu	grain protein	grpp	plant height	plnht
amylose content	amylose	days to flag leaf senescence	dfls	grain weight	grwgt	plot shattering	plsh
As	As	days to heading	dLh	grain weight per head	grwh	plump grain	plng
avenanthramide 2c	aven2c	days to heading (fall planting)	dLh_f	grain width	grwid	polyphenol oxidase activity	pxo
avenanthramide 2f	aven2f	delta-tocopherol	dL-tocp	grain yield	grwy	powdery mildew (0-9)	pm
avenanthramide 2p	aven2p	delta-tocotrienol	dL-tct	grain yield (main tillers)	grwy_mnt	powdery mildew incidence	pmi
avenanthramide 5p	aven5p	diastatic power	dsp	harvest index	hvi	powdery mildew reaction type	pmrt
avenanthramide total	aven_t	DON	DON	heading date	hdn_dt	productive tillers per plant	ptpp
awn type	awn_type	Fs	Fs	heading date (Julian)	hdn_dt_j	residual beta-glucanase	rB-g
bacterial leaf streak	bas_ll_str	fertile spikelets per head	fsh	K	K	S	S
basal sheath spikelets per head	bassh	FHB incidence	FHB_I	kernal weight	kww	seeds per head	slph
beta glucan	br_gl	FHB severity	FHB_S	kernals per spike	kpps	single kernel weight	skkw
beta glucan dwb	br_gl_dwb	flag leaf angle	fla	leaf chlorophyll content	lfc	soluble protein/ total protein	stpp
beta-glucanase activity	br_gla	flag leaf angle T1	fla_T1	leaf rust (0-9)	lr	spike angle	slpa
beta-glucanase thermostability	br_gla_t	flag leaf chlorophyll content	flc	leaf rust reaction type	lrrt	spike density	slpd
beta-tocopherol	br_tocp	flag leaf chlorophyll content T1	flc_T1	leaf rust response	lrr	spike exertion	slpe
beta-tocotrienol	br_toct	flag leaf chlorophyll content T2	flc_T2	leaf rust severity	lrs	spike length	slpl
biomass at maturity	bm_mam	flag leaf length	ll	Li	Li	spike number	slpn
broadens grain protein	br_gp	flag leaf stay-green period	flsgp	lodging	lmg	spikelets per head	slph
broadens plump grain	br_pg	flag leaf width	flw	lodging degree	lmgd	spikelets per panicle	slpp
Ca	Ca	flowering date	flw_d	lodging incidence	lmg_i	spikes per area	slps
canopy senescence score T1	csT1	forage protein	frg_p	lodging severity	lmg_s	spot blotch severity	slbs
canopy senescence score T2	csT2	forage yield	frg_y	mult beta-glucan	mb_b_g	stem diameter	stnd
canopy senescence score T3	csT3	free amino nitrogen	fan	mult extract	mb_e	stem length	stnl
canopy senescence score T4	csT4	frozen injury	fzi	mult protein	mb_p	stem rust coefficient of infection	srcof
canopy senescence score T5	csT5	gamma-tocopherol	gm-tcp	maturity date	mat_dt	stem rust infection response	srir
canopy senescence score T6	csT6	gamma-tocopherol + beta-tocotrienol	gt_btc	maturity date (physiological)	mat_dpy	stem rust severity	srms
canopy senescence score T7	csT7	gamma-tocotrienol	gm-tct	Mg	Mg	stem solubness	stms
canopy temperature (grain fill)	ct_gf	gloomy sheath	glsh	Mo	Mo	sterile spikelets per head	slsp
canopy temperature depression (flowering)	ct_dfl	gloomy spike	glsp	Mo	Mo	striae breakage	stbr
canopy temperature depression (grain fill)	ct_dgf	glume pubescence	glmp	Ni	Ni	stripe rust infection type (0-9)	NDVI
							Zn

Fig. S4 Triticale data sets: Combining the phenotypic correlation matrices from oat (78 correlation matrices), barley (143 correlation matrices) and wheat (144 matrices) data sets downloaded and selected in a similar way as in Example 4 were combined to obtain the DAG involving 196 traits.

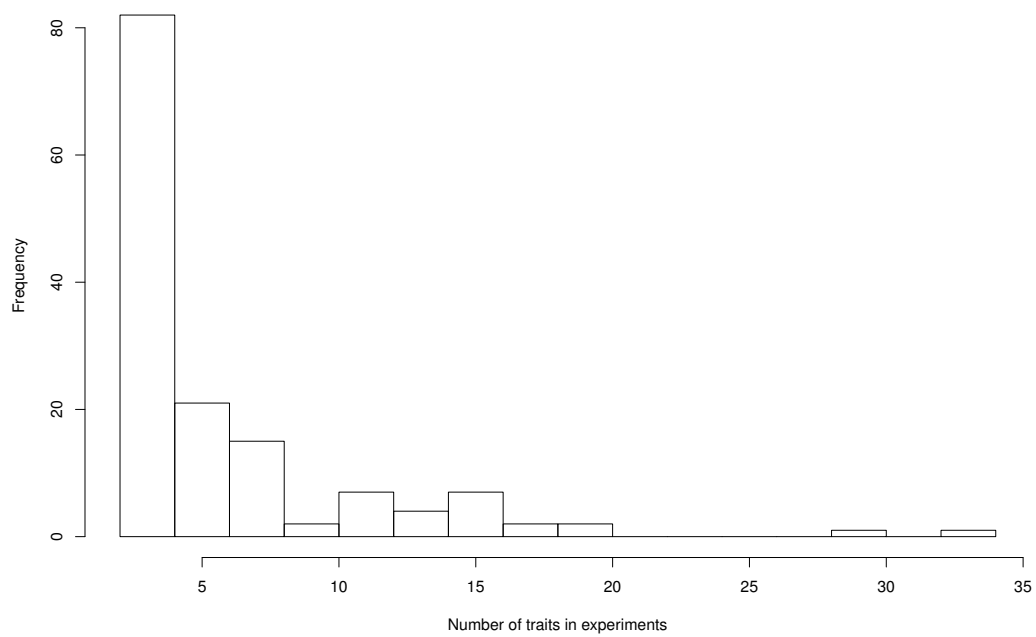


Fig. S5 Triticale data set: The distribution of the numbers of traits in 144 phenotypic trials at Triticale Toolbox for wheat. The mean and the median of the number of traits in these trials were 5.9 and 4 correspondingly.

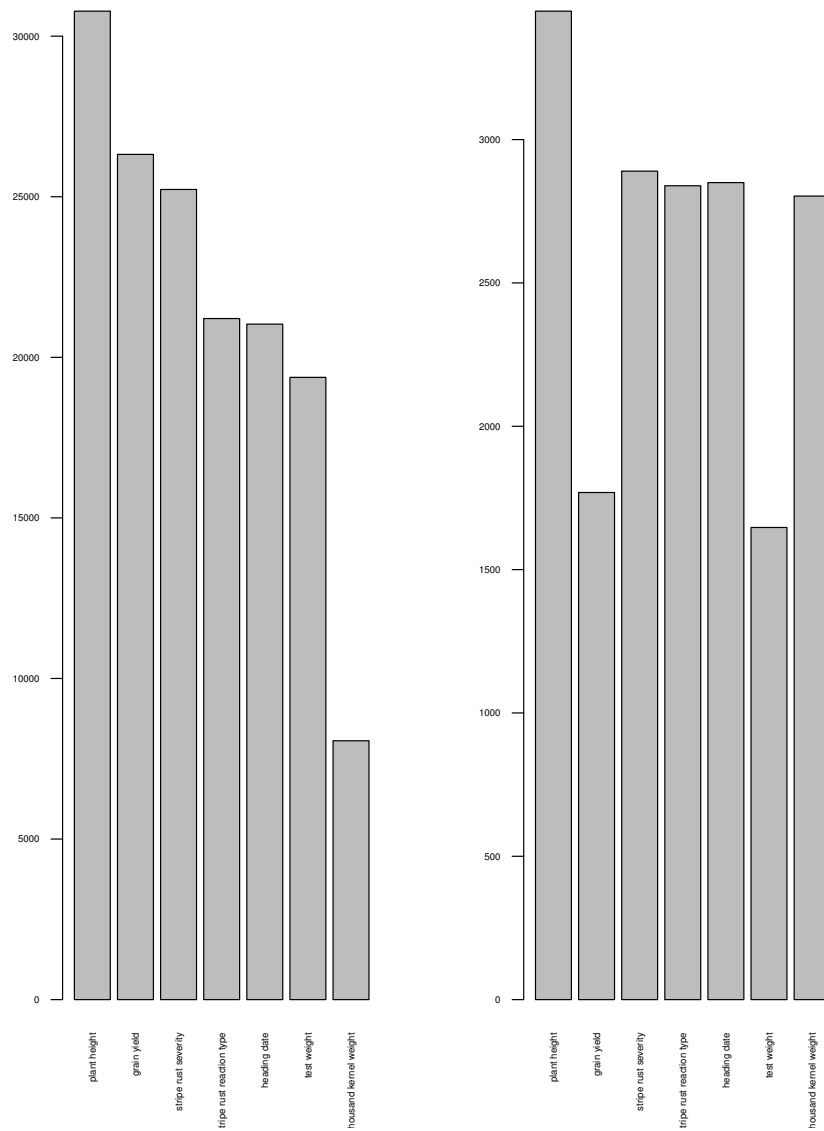


Fig. S6 Triticale data set: Number of phenotypic observations (left) and the number of genotypes available in Triticale Toolbox for a set of 7 selected traits for the 9102 genotypes in the combined relationship matrix.